Response of a Compressible, Turbulent Boundary Layer to a Short Region of Surface Curvature

David Degani*
Technion—Israel Institute of Technology, Haifa, Israel
and
Alexander J. Smits†
Princeton University, Princeton, New Jersey

Calculations were performed to investigate the supersonic flow of a turbulent boundary layer over short regions of concave surface curvature. Upstream of each curved surface the freestream Mach number was 2.9. Three different constant radii of curvature models were investigated to cover a range of curvatures and turning angles. The numerical technique solved the full, Reynolds-averaged Navier-Stokes equations using two different turbulence models: algebraic eddy viscosity model and a one-equation model. The calculations were compared with recent experimental data and the agreement was surprisingly good, especially for the computations using the one-equation model.

I. Introduction

IN this investigation, we calculate the behavior of a supersonic turbulent boundary layer experiencing a short region of concave surface curvature. Within the curved region, the boundary layer experiences the combined effects of an adverse pressure gradient, bulk compression, and concave streamline curvature.

Longitudinal curvature, bulk compression, longitudinal pressure gradient, and streamline divergence are examples of what Bradshaw[1] called "extra" strain rates, that is, strain rates additional to the main shear $\partial U/\partial y$. Experience has shown that even relatively small extra strain rates can have very significant effects on the flow behavior. For instance, a small amount of concave curvature in a zero-pressure-gradient, subsonic flow amplifies the turbulence levels strongly, increases the turbulence length scales, and produces longitudinal roll cells through a Taylor-Goertler-like instability.[2-4] In a supersonic flow, similar effects appear to occur. For example, Thomann[5] obtained heat-transfer data for a zero-pressure-gradient, Mach 2.5 turbulent boundary layer on a concavely curved wall and found that even weak curvature dramatically increased the heat-transfer rates.

Little is known, however, regarding the simultaneous action of different extra strain rates. They appear to interact strongly, and the interaction can be extremely complex. For example, Smits et al.[6] found that a boundary layer experiencing the simultaneous effects of concave curvature and streamline divergence did not exhibit the turbulence amplification expected if each effect were added linearly. Nor did the boundary layer show any evidence for the presence of longitudinal roll cells (see also Smits and Joubert[7] and Smits and Wood[8]). These studies indicated that the amplification of longitudinal vorticity by concave curvature and the amplification of spanwise vorticity by divergence interact nonlinearly to prevent the formation of steady longitudinal vortices.

In the present case of a compressible flow over a concavely curved wall, curvature acts in combination with the bulk compression and longitudinal pressure gradient. Similar flow geometries were investigated by McLafferty and Barber,[9] Hoydysh and Zakkay,[10] Chou and Childs,[11] and especially Sturek and Danberg[12,13] and Laderman.[14] The results, however, gave little indication regarding the relative influence of each effect, and they provided little insight into the effect of perturbation rate.

Previous calculations of compressible flows with streamline curvature are limited in number. The early work by Bradshaw[15] was restricted to plane walls with adverse pressure gradients, and later work has usually focused on the computation of shock-wave/boundary-layer interactions.[16,17] The Sturek-Danberg flow, however, has been calculated by several workers, and the results were summarized by Rubesin et al.[18] The turbulence models used in these calculations ranged from a simple mixing length relationship to a full Reynolds stress model, and the results were rather contradictory. For example, the mixing length model predicted the mean velocity profiles fairly well, but the agreement with the skin-friction distribution was poor. Yet, the Reynolds stress model gave precisely the opposite results. When taken as a whole, these calculations demonstrate how difficult it is to predict complex, compressible flows.

To improve our understanding of curved, compressible flows, Taylor and Smits[19] recently tested the three models shown in Fig. 1. For model 1, the ratio of initial boundary-layer thickness to radius of curvature δ_0/R was 0.1, and the turning angle was fixed at 8 deg; for model II, δ_0/R was 0.02, and the turning angle was 8 deg; and for model III, δ_0/R was 0.02, and the turning angle was 16 deg. Further experimental details may be found in Taylor.[20]

These three experiments tested the response of the boundary layer to a wide range of stress gradients and strain rates. This range is illustrated in Fig. 2, where the magnitudes of the pressure gradient, compression, and curvature are qualitatively shown. The area under each curve represents the overall pressure rise, density change, and total turning angle for each model. By examining a range of perturbation rates and strengths, the experiments serve as an excellent test case for turbulence models.

Two different turbulence models were used in the current calculations: the algebraic eddy viscosity model due to Baldwin and Lomax[21] and the one-equation model due to Rube-

Presented as Paper 85-1667 at the AIAA 18th Fluid Dynamics and Plasmadynamics and Lasers Conference, Cincinnatti, OH, July 16-18, 1985; received Nov. 19, 1986; revision received April 27, 1988.

*Associate Professor, Faculty of Mechanical Engineering. Member AIAA.
†Associate Professor, Department of Mechanical and Aerospace Engineering. Member AIAA.

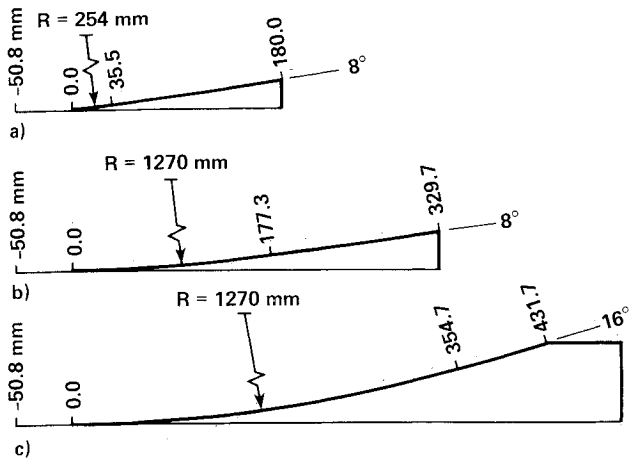

Fig. 1 Test model geometries: a) model I; b) model II; and c) model III (R is the longitudinal radius of curvature).

sin.[22] The Baldwin-Lomax model was chosen because of its widespread use in compressible flow calculations, particularly where the boundary conditions are changing rapidly (see, for example, Visbal and Knight[23]). The version of the Rubesin model used here is due to Viegas and Coakley,[16] and it introduces an elementary history effect into the calculations. The models were used in a numerical solution of the full, Reynolds-averaged Navier-Stokes equations using an implicit approximate factorization finite-difference algorithm. Neither turbulence model takes explicit account of direct curvature and compressibility effects on the turbulence. Recent unpublished computations by Fernando and Donovan at Princeton, using the boundary-layer code developed by Bradshaw,[24] indicated that the empirical corrections required to take account of the compressibility effects were significant in that case. Here, we use the Reynolds-averaged Navier-Stokes equations, and one of the aims of these calculations is to determine the need for empirical extra strain-rate corrections in this context. Further details of the numerical scheme are given in Sec. II and III.

The results of the calculation are compared with experimental data in Sec. IV, and a discussion and conclusions are presented in Sec. V.

II. Governing Equations

The strong conservation law form of the Navier-Stokes equations in general coordinates can be written in nondimensional form as

$$\frac{\partial \hat{q}}{\partial \tau} + \frac{\partial \hat{E}}{\partial \xi} + \frac{\partial \hat{F}}{\partial \eta} = Re^{-1}\left[\frac{\partial}{\partial \xi}(\hat{R}^{\xi} + \hat{R}^{\eta}) + \frac{\partial}{\partial \eta}(\hat{S}^{\xi} + \hat{S}^{\eta})\right] \tag{1}$$

The inviscid flux vectors in Eq. (1) are

$$\hat{q} = \bar{q}/J$$

$$\hat{E} = (\xi_t \bar{q} + \xi_x \bar{E} + \xi_y \bar{F})/J$$

$$\hat{F} = (\eta_t \bar{q} + \eta_x \bar{E} + \eta_y \bar{F})/J \tag{2}$$

and the viscous flux vectors are

$$\hat{R} = \hat{R}^{\xi}(\bar{q}, \bar{q}_{\xi}) + \hat{R}^{\eta}(\bar{q}, \bar{q}_{\eta}) = (\xi_x \bar{R} + \xi_y \bar{S})/J$$

$$\hat{S} = \hat{S}^{\xi}(\bar{q}, \bar{q}_{\xi}) + \hat{S}^{\eta}(\bar{q}, \bar{q}_{\eta}) = (\eta_x \bar{R} + \eta_y \bar{S})/J \tag{3}$$

where $\bar{E}$, $\bar{F}$, $\bar{R}$, and $\bar{S}$ are the flux vectors in Cartesian coordinates, and J the transformation Jacobian.

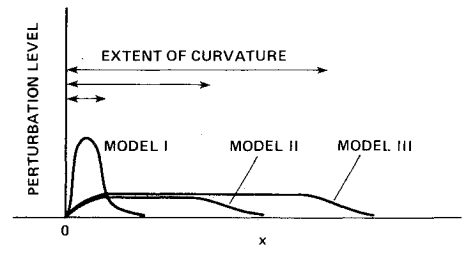

Fig. 2 Qualitative distribution of longitudinal pressure gradient, ratio of boundary-layer thickness to longitudinal radius of curvature, and compression term ($= -\nabla V$), along a streamline originating at $y/\delta_0 = 0.5$.

An implicit approximate factorization finite-difference algorithm is used to solve Eq. (1). Further details of the numerical technique and the treatment of the boundary and initial conditions may be found in Refs. 25 and 26. Briefly, a 120×48 grid was used for all calculations, and the resolution near the wall was maintained such that the mesh size normal to the wall was less than $5\nu/u_{\tau}$. The grid spacing in the streamwise direction was fine in the curvature region ($\Delta x/\delta_0 = 0.045$) and stretched to a coarser grid [$(\Delta x/\delta_0)_{\max} = 0.64$] up- and downstream of the curvature region.

III. Viscosity Models

Sutherland's law is used to calculate the laminar viscosity. The effects of turbulence are simulated in terms of an eddy viscosity coefficient, using a zero- and a one-equation turbulence model.

Zero-Equation Model

For the zero-equation model, the Baldwin-Lomax algebraic model[21] is used. Here, the laminar flow coefficients are replaced by

$$\mu = \mu_l + \mu_t, \qquad \frac{\kappa}{c_p} = \frac{\mu_l}{Pr} + \frac{\mu_t}{Pr_t} \tag{4}$$

In the Baldwin-Lomax formulation, μ_t is given by

$$\begin{aligned} \mu_t &= (\mu_t)_{\text{inner}} \qquad y \le y_c \\ \mu_t &= (\mu_t)_{\text{outer}} \qquad y > y_c \end{aligned} \tag{5}$$

where y is the local distance measured normal to the body surface, and y_c is the smallest value of y at which the values from the inner and outer region formulas are equal. Within the inner region,

$$(\mu_t)_{\text{inner}} = \rho l^2 |\omega| \tag{6}$$

where

$$l = ky[1 - e^{-(y^+/A^+)}]$$

$|\omega|$ is the magnitude of the local vorticity vector, and $y^+ = (\sqrt{\rho_w \tau_w}/\mu_w)y$.

In the outer region, for attached boundary layers, the turbulent viscosity coefficient is given by

$$(\mu_t)_{\text{outer}} = KC_{cp}\rho F_{\text{wake}} F_{\text{Kleb}}(y) \tag{7}$$

In Eq. (7), K and C_{cp} are constants, F_{Kleb} is the Klebanoff intermittency factor, and

$$F_{\text{wake}} = y_{\max} F_{\max} \tag{8}$$

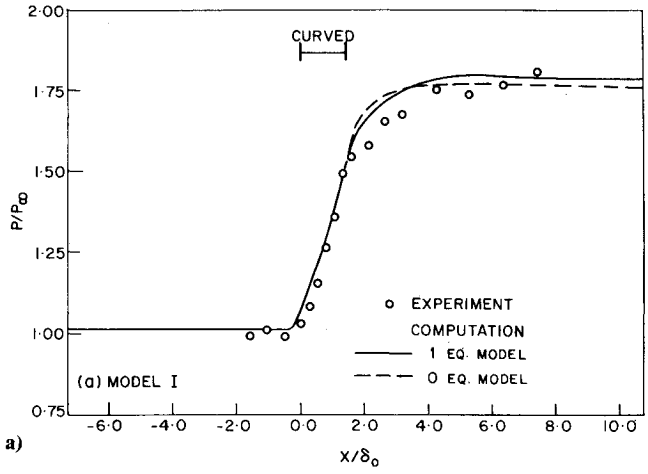

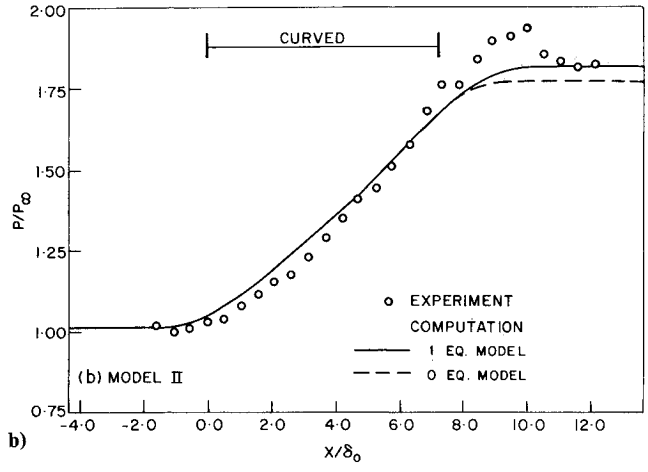

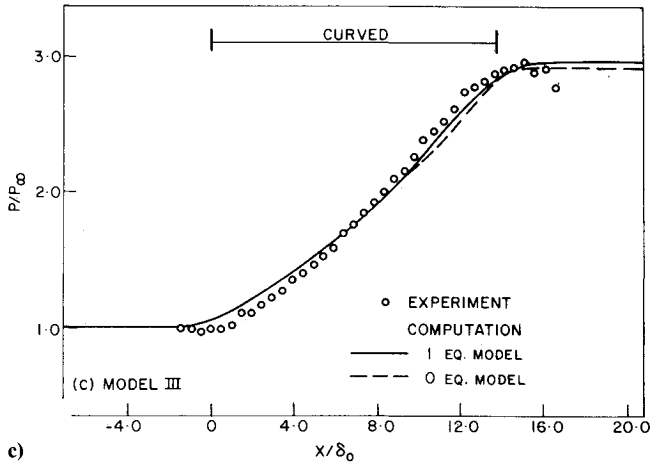

Fig. 3 Comparison between calculated and experimental pressure distributions: a) model I; b) model II; and c) model III.

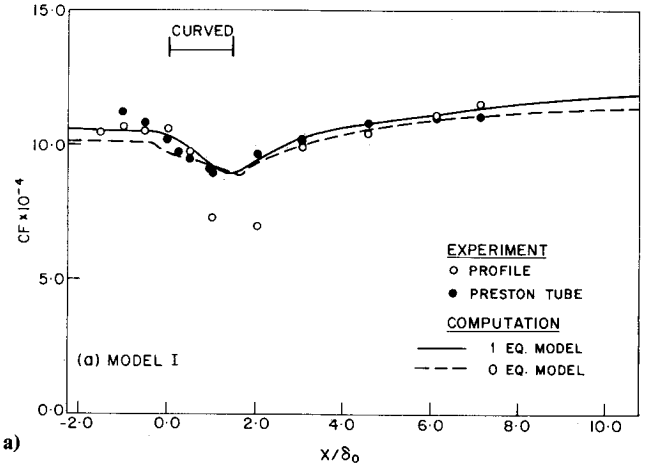

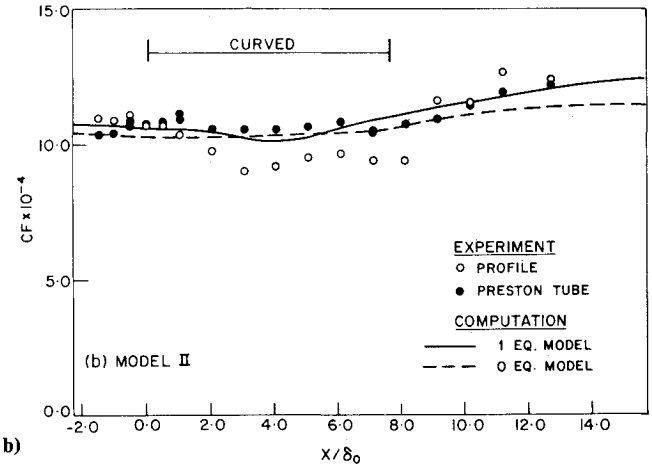

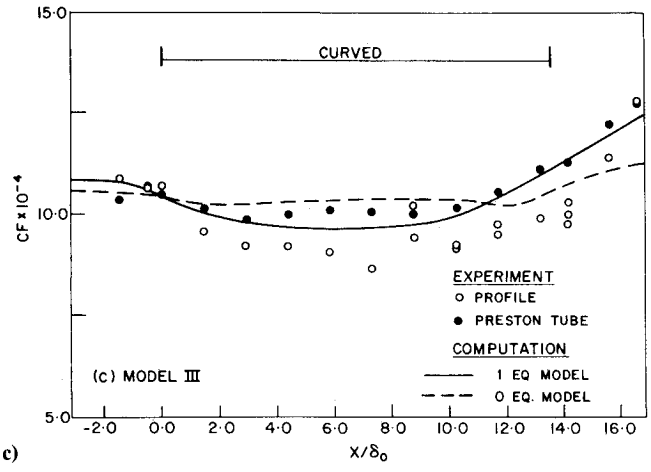

Fig. 4 Comparison between calculated and experimental skin-friction coefficient distributions: a) model I; b) model II; and c) model III.

where F_{max} is the maximum value that the function $F(y)$, defined as

$$F(y) = |\omega| y \, [1 - e^{-(y^+/A^+)}] \tag{9}$$

takes in a local profile, and y_{max} is the value of y at which F_{max} occurs. The constants appearing in Eqs. (4-9) are

$$Pr = 0.72 \qquad A^+ = 26 \qquad K = 0.0168$$

$$Pr_t = 0.9 \qquad k = 0.4 \qquad C_{cp} = 1.6 \tag{10}$$

One-Equation Model

The one equation model (or kinetic energy equation model) uses an additional partial-differential equation to calculate the eddy viscosity coefficients. The model used in the present work was formulated by Rubesin[22] for compressible flows, based on the Glushko[27] model for incompressible flat-plate boundary-layer flows. Coakley et al.[17] used a simpler version of Rubesin's model where certain compressibility terms involving first derivatives of the temperature were omitted. (These terms were found to have a negligible effect by Viegas and Coakley.[16]) This model has one turbulence source func-

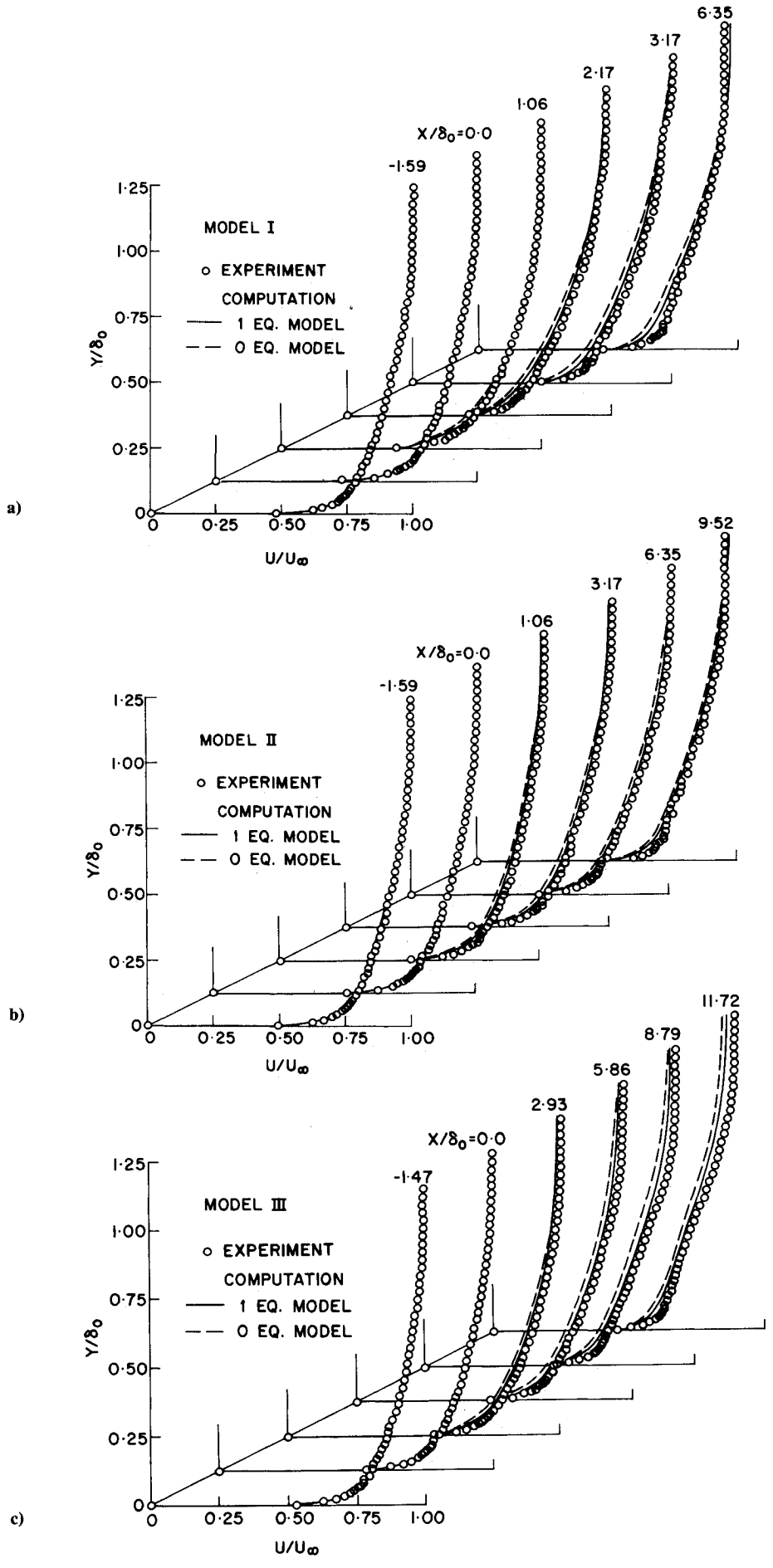

Fig. 5 Comparison between calculated and experimental velocity profiles: a) model I; b) model II; and c) model III.

tion H_k:

$$H_k = \mu_t S^2 - 2\rho k D/3 - C\mu_k k/L^2 \qquad (11)$$

where

$$S^2 = (u_y + v_x)^2 + 2[u_x^2 + v_y^2 + (v/r)^2] - 2D^2/3$$

$$D = u_x + v_y + v/r$$

$$\mu_t = \alpha\mu_l R_t \tilde{H}(R_t/R_0)$$

$$R_t = \rho\sqrt{k}\, L/\mu_l$$

$$\tilde{H}(\tilde{R}) = \tilde{R} \qquad \text{for } \tilde{R} < 0.75$$

$$= \tilde{R} - (\tilde{R} - 0.75)^2 \qquad \text{for } 0.75 \le \tilde{R} \le 1.25$$

$$= 1 \qquad \text{for } 1.25 < \tilde{R}$$

$$\alpha = 0.2,\ C = 3.93,\ R_0 = 110,\ Pr_k = 2.5$$

Here k is the turbulence kinetic energy, $k = \overline{\rho u_i' u_i'}/2\bar{\rho}$, and L is the length scale as specified by Glushko[27]:

$$L/\delta = y/\delta \qquad \text{for } 0 \le y/\delta < 0.23$$

$$= \frac{(y/\delta + 0.37)}{2.61} \qquad \text{for } 0.23 \le \frac{y}{\delta} < 0.57$$

$$= \frac{(1.48 - y/\delta)}{2.52} \qquad \text{for } 0.57 \le \frac{y}{\delta} \le 1.48 \qquad (12)$$

The total kinetic energy diffusivity μ_k is given by

$$\mu_k = \mu_l + \mu_t/Pr_k \qquad (13)$$

The total viscosity μ and the thermal energy diffusivity are as in Eq. (4).

IV. Results

To obtain the initial profile for the computations, the flow on a flat plate was calculated and adjusted until the upstream Reynolds number based on boundary-layer thickness matched the value observed in the experiment. For both the computations and the experiment, the stagnation pressure was 6.9×10^5 Pa (100 psia), and the incoming flow had a freestream Mach number of 2.87 with a unit Reynolds number of 6.3×10^7/m. The wall conditions were assumed to be adiabatic. The incoming turbulent boundary layer developed in a zero pressure gradient, and just upstream of each model the boundary-layer thickness δ_0 was 26 mm.

The x coordinate was defined as the streamwise direction and was measured along the surface of the model with the origin at the beginning of curvature. The y coordinate was measured normal to the wall.

The calculated wall static pressures are compared with the experimental values in Fig. 3. The results show good qualitative agreement, but quantitatively the agreement is not so satisfactory. For example, the calculation does not reproduce the rather slow pressure rise observed in the model I experiment downstream of the curvature, and the pressure gradients for model III are underestimated. The two turbulence models give almost identical results in the curved region, but in every case the one-equation model predicts a slightly higher downstream level. The differences, however, are not significant, and the two calculations bracket the isentropic value.

The skin-friction distributions are shown in Fig. 4. The results for both turbulence models demonstrate excellent agreement with experiment in the curved regions of all three flows, especially when we note that the experimental uncertainty in the absolute value of C_f in these regions is about

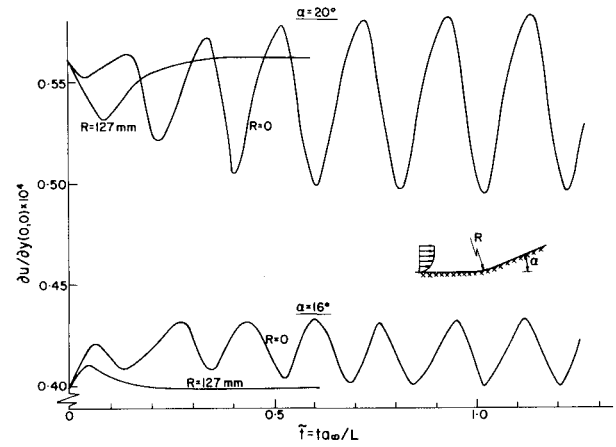

Fig. 6 Oscillations in the calculated velocity gradient as a function of the nondimensionalized time.

±15% and that the Preston tube values are probably more reliable than those deduced from the velocity profiles. (The principal difficulty in deducing C_f values in strongly perturbed supersonic flows seems to lie in defining the correct boundary-layer edge conditions. In the present case, this uncertainty significantly affects the accuracy of the values derived from the velocity profile in the region of rapid pressure rise.[28]) Downstream in the recovery zone, however, the one-equation model becomes more obvious as the perturbation strength and duration increase; this trend demonstrates the importance of including flow history effects in the calculation.

The calculated and experimental velocity profiles, shown in Fig. 5, agree closely in the outer part of the layer, that is, for $y/\delta > 0.2$. The differences between the two turbulence models are not really significant because the maximum experimental uncertainty is about ±5%, whereas the calculations agree with the data to within 3–4%. Near the wall, the computations do not reproduce the "kinks" observed in the experimental profiles. When plotted in log-law coordinates, these kinks show up as "dips" below the log law, suggesting an increase in the turbulence length scale.[4,6] Both turbulence models have a fixed length scale distribution, however, and cannot be expected to reproduce these dips below the log law.

Similar calculations for a separated, shock-wave/boundary interaction were presented by Degani and Steger.[25] They reported that a small perturbation introduced into the flowfield caused the separation bubble to oscillate at almost constant amplitude and frequency (about 2500 Hz). It was thought to be due to a numerical interaction between the turbulence model and the flowfield (Fig. 6, $\alpha = 20$ deg and $R = 0$).

Repeating this case using the two turbulence models considered here showed only small differences among the models. However, when the radius of the corner was changed to $R = 127$ mm, the perturbation was damped to a steady state (Fig. 6). The 16-deg case gave similar results; that is, oscillations were observed for $R = 0$ at about the same frequency as observed in the 20-deg case but with a lower amplitude, and damped oscillations were observed for $R = 127$ mm (Fig. 6). Similar oscillations were observed experimentally[29,30] at about the same frequency, and it is possible that the numerical results are physically valid.

The fact that the frequencies observed in the two cases (16 and 20 deg) are about the same is to be expected, since the only characteristic length is the boundary layer thickness upstream of the bubble (which is about the same for both cases), and the corresponding Strouhal number, $St = f\delta_0/U_\infty$, is approximately constant.

V. Discussion and Conclusions

The results demonstrate that a one-equation model is superior to an algebraic eddy viscosity model for the calculation of

curved, compressible flows. This conclusion holds over a range of perturbation intensities and duration, although for some quantities (such as the mean velocity) the differences between the models are not significant. Relative to the calculations of the Sturek-Danberg flow reported by Rubesin et al.,[18] the performance of the algebraic model in the current computations was generally better than the performance of the mixing length model, whereas the one-equation results presented here were considerably better than any of the calculations summarized by Rubesin et al.

The relative success of these Reynolds-averaged Navier-Stokes calculations strongly suggest that the need for empirical modifications to the turbulence length scale distribution, commonly used to account for curvature and compressibility effects,[24] is partly driven by the use of the boundary-layer approximation. The present calculations also lead to interesting implications for the computation of shock-wave/boundary-layer interactions. The mean flow measurements in models I and II were recently complemented by a complete set of turbulence measurements.[31] In the region downstream of the curved wall, the mean and turbulent flow behavior for model I was very similar to that observed downstream of the interaction zone in the corresponding 8-deg compression corner flow, with the same incoming boundary layer. Jayaram et al.[31] speculated that model I and the compression corner can be classed as "rapid" perturbations, in that the flow behavior appears to depend only on the total strain applied rather than on the detailed nature of the strain field. Thus, we predict that the one-equation turbulence model used here should perform reasonably well in calculations of compression corner flows, as long as the shock is not strong enough to produce a major entropy increase, separation, or significant unsteadiness. Work in this area is currently in progress.

Acknowledgment

NASA Ames Research Center provided financial support for the first author and the computational facilities for the calculations. The second author received support form NASA Langley Research Center under Grant NAG-1-545 during the course of this work.

References

[1]Bradshaw, P., "Effects of Streamline Curvature on Turbulent Flows," AGARDograph 169, Aug. 1973.

[2]So, R. M. and Mellor, G. L., "An Experimental Investigation of Turbulent Boundary Layers Along Curved Surfaces," NASA CR-1940, April 1972.

[3]Ramaprian, B. R. and Shivaprasad, B. G., "The Structure of Turbulent Boundary Layers Along Mildly Curved Surfaces," *Journal of Fluid Mechanics,* Vol. 85, 1978, pp. 273-303.

[4]Smits, A. J., Young, S. T. B., and Bradshaw, P., "The Effect of Short Regions of High Surface Curvature on Turbulent Boundary Layers," *Journal of Fluid Mechanics,* Vol. 94, 1979, pp. 209-242.

[5]Thomann, H., "Effect of Streamwise Curvature on Heat Transfer in a Turbulent Boundary Layer," *Journal of Fluid Mechanics,* Vol. 33, Pt. 2, 1968, pp. 283-292.

[6]Smits, A. J., Eaton, J. A., and Bradshaw, P., "The Response of Turbulent Boundary Layer to Lateral Divergence," *Journal of Fluid Mechanics,* Vol. 94, 1979, pp. 243-268.

[7]Smits, A. J. and Joubert, P. N., "Turbulent Boundary Layers on Bodies of Revolution," *Journal of Ship Research,* Vol. 26, 1982, pp. 135-147.

[8]Smits, A. J. and Wood, D. H., "The Response of Turbulent Boundary Layers to Sudden Perturbations," *Annual Reviews of Fluid Mechanics,* Vol. 17, 1985, pp. 321-358.

[9]McLafferty, G. H. and Barber, R. E., "The Effect of Adverse Pressure Gradient on the Characteristics of Turbulent Boundary Layers in Supersonic Streams," *Journal of the Aerospace Sciences,* Vol. 29, Jan. 1969, pp. 1-10.

[10]Hoydysh, W. G. and Zakkay, V., "An Experimental Investigation of Hypersonic Turbulent Boundary Layers in Adverse Pressure Gradient," *AIAA Journal,* Vol. 7, Jan. 1969, pp. 105-116.

[11]Chou, J. H. and Childs, M. E., "An Experimental Study of Surface Curvature Effects on a Supersonic Turbulent Boundary Layer," AIAA Paper 83-1672, 1983.

[12]Sturek, W. B. and Danberg, J. E., "Supersonic Turbulent Boundary Layer in an Adverse Pressure Gradient. Part I: The Experiment," *AIAA Journal,* Vol. 10, April 1972, pp. 475-480.

[13]Sturek, W. B. and Danberg, J. E., "Supersonic Turbulent Boundary Layer in an Adverse Pressure Gradient, Part II: Data Analysis," *AIAA Journal,* Vol. 10, May 1972, pp. 630-636.

[14]Laderman, A. J., "Adverse Pressure Gradient Effects on Supersonic Boundary Layer Turbulence," *AIAA Journal,* Vol. 18, Oct. 1980.

[15]Bradshaw, P., "The Effect of Mean Compression or Dilatation on the Turbulence Structure of Supersonic Boundary Layers," *Journal of Fluid Mechanics,* Vol. 63, 1974, pp. 449-464.

[16]Viegas, J. R. and Coakley, T. J., "Numerical Investigation of Turbulence Models for Shock Separated Boundary-Layer Flows," AIAA Paper 77-44, Jan. 1977.

[17]Coakley, T. J., Viegas, J. R., and Horstman, C. C., "Evaluation of Turbulence Models for Three Primary Types of Shock Separated Boundary Layers," AIAA Paper 77-692, June 1977.

[18]Rubesin, M. W., Crisalli, M. J., Lanfranco, M. J., Horstman, C. C., and Acharya, M., "A Critique of Some Recent Second-Order Turbulence Closure Models for Compressible Boundary Layers," AIAA Paper 77-128, Jan. 1977.

[19]Taylor, M. and Smits, A. J., "The Effects of a Short Region of Concave Curvature on a Supersonic Turbulent Boundary Layer," AIAA Paper 84-0169, 1984.

[20]Taylor, M. W., "A Supersonic Turbulent Boundary Layer on Concavely Curved Surfaces," Princeton Univ., Princeton, NJ, MAE Rept. 1684, Sept. 1984.

[21]Baldwin, B. S. and Lomax, H., "Thin Layer Approximation and Algebraic Model for Separated Turbulent Flow," AIAA Paper 78-257, 1978.

[22]Rubesin, M. W., "One-Equation Model of Turbulence for Use with the Compressible Navier-Stokes Equations," NASA TM X-73-128, April 1976.

[23]Visbal, M. R. and Knight, D. D., "Evaluation of the Baldwin-Lomax Turbulence Model for Two-Dimensional Shock Wave Boundary Layer Interactions," AIAA Paper 83-1697, 1983.

[24]Bradshaw, P., "The Effect of Mean Compression or Dilatation on the Turbulence Structure of Supersonic Boundary Layers," *Journal of Fluid Mechanics,* Vol. 63, 1974, pp. 449-464.

[25]Degani, D. and Steger, J. L., "Comparison Between Navier-Stokes and Thin-Layer Computations for Separated Supersonic Flow," *AIAA Journal,* Vol. 21, Nov. 1983, pp. 1604-1606.

[26]Degani, D., "Numerical Algorithm Conjugating Steady and Transient, Separated, Compressible Flow and a Solid Body Having Arbitrarily Distributed Heat Sources," *Numerical Heat Transfer,* Vol. 7, 1984, pp. 395-411.

[27]Glushko, G. S., "Turbulent Boundary Layer on a Flat Plate in an Incompressible Fluid," *Bulletin of the Academy of Sciences of the USSR, Mechanical Series,* No. 4, 1965, pp. 13-23.

[28]Fernando, E. M., Donovan, J. F., Smith, D. R., and Smits, A. J., "Conventional Skin Friction Measurement Techniques for Strongly Perturbed Supersonic Turbulent Boundary Layers," Second AIAA Shear Flow Control Conference, Tempe, AZ, March 1989, (submitted for presentation).

[29]Dolling, D. S. and Murphy, M., "Wall Pressure Fluctuations in a Supersonic Separated Compression Ramp Flowfield," AIAA Paper 82-0986, 1982.

[30]Andreopoulos, J. and Muck, K. C., "Some New Aspects of the Shock Wave Boundary Layer Interaction in Compression Ramp Flows," AIAA Paper 86-0342, 1986.

[31]Jayaram, M., Taylor, M. W., and Smits, A. J., "The Response of a Compressible Turbulent Boundary Layer to Short Regions of Concave Surface Curvature," *Journal of Fluid Mechanics,* Vol. 175, 1987, pp. 343-362.